

# Statistical analysis of turbulent flux and intermittency in the nonfusion magnetoplasma Blaamann

A. Fredriksen

*Auroral Observatory of Tromsø, N-9036 Tromsø, Norway*

C. Riccardi, L. Cartegni, D. Draghi, and R. Trasarti-Battistoni

*Dipartimento di Fisica, Università di Milano-Bicocca and INFN, Piazza della Scienza 3, I-20126 Milano, Italy*

H. E. Roman

*Dipartimento di Fisica, Università di Milano, Via Celoria 16, 20133 Milano, Italy*

(Received 14 May 2003; accepted 27 August 2003)

Turbulent particle flux due to correlated fluctuations of density and  $\vec{E} \times \vec{B}$ -drift velocity has been statistically characterized in the simple magnetized torus Blaamann [F. J. Øynes, O. M. Olsen, H. L. Pécseli, A. Fredriksen, and K. Rypdal, *Phys. Rev. E* **57**, 2242 (1998)]. The shape and width of the probability distribution functions (PDF) and how they change as a function of time resolution  $\tau$  upon coarse-graining have been analyzed. The shape of the PDF is non-Gaussian with a sharp central peak and is strongly asymmetric. The resulting width,  $\sigma$ , scales as a power-law over about two decades in  $\tau$ ,  $\sigma \sim \tau^H$ , for  $\tau > 100 \mu\text{s}$ . As  $\tau$  decreases the width tends to flatten, i.e., the effective Hurst exponent  $H$  increases continuously in the interval  $0.5 < H < 1$ . The behavior of the PDF at small time scales seems to be ascribed to the presence of coherent structures, living in the torus generated by flux instability. © 2003 American Institute of Physics. [DOI: 10.1063/1.1619977]

## I. INTRODUCTION

Self-similarity, universality and scale-invariance are general properties of the turbulence in fluids and plasmas. Recently many papers on statistical analysis have been devoted to understanding the properties of turbulence and turbulent transport in magnetically confined plasmas.<sup>1-7</sup> The main aim has been to study and characterize the intermittent properties of plasma parameters and their differences—similarities between different magnetically confined plasmas. Some works have also been devoted to testing the self-organized criticality paradigm in transport processes and to search for avalanche-like processes, like burst behavior and long range and long distance correlations.

In this paper, we approach the analysis of the turbulent transport through a statistical analysis of the probability distribution functions (PDF)<sup>6</sup> in order to better understand the strong intermittent particle turbulent transport in a simple magnetized torus, and its relationship with the dynamics of the turbulent processes. We analyze systematically power-law scaling, self-similarity, non-Gaussian properties, and intermittency of turbulent fluctuations, relating them to the long-lived structures<sup>8</sup> observed in Blaamann. It is found that full information over the whole range of radial distances inside the torus and the simultaneous study of different physical quantities are required to understand the physics involved. The comparison between the statistical properties of Blaamann and those of other devices of different sizes and magnetic configurations, like fusion devices, is also performed in order to search for possible universal properties of the turbulence in magnetized plasmas.

We start in Sec. II with a brief discussion of the equip-

ment set up, followed by a description of the method in Sec. III. The results and their discussion are presented in Sec. IV, and our main conclusions summarized in Sec. V.

## II. EQUIPMENT SETUP

Blaamann is a simple, steady-state magnetized torus.<sup>9</sup> Details of the experimental setup, plasma production and typical plasma parameters can be found in the paper of Øynes *et al.*<sup>9</sup> In this work, turbulence has been experimentally investigated at a helium neutral gas pressure of  $10^{-4}$  mbar along the entire plasma radius. Discharge plasma parameters are: filament current 100 A, voltage bias 160 V, toroidal magnetic field 1440 G, and discharge plasma current of 1 A. The turbulent particle flux  $\Gamma$  is directly related to correlated temporal fluctuations of plasma density  $\bar{n}$  and fluid velocity  $\bar{u}$ , which can be expressed in terms of the directly measurable quantities by a Langmuir probe.

A Langmuir probe composed of three pins was used to measure the poloidal electric field and the plasma density fluctuations. The two pins for the electric field measurements were placed at the same radial and toroidal coordinates but poloidally displaced by a known distance  $d = 1$  cm. The third pin was placed along the same radial and poloidal coordinate as one of the other two, but displaced by 1 cm in the toroidal direction to measure the ion saturation current.

In this way, we simultaneously measured the ion saturation current,  $I_{\text{sat}}$ , and the floating potential  $V_f$ , as functions of time. The instantaneous values of the plasma potential  $V_p$  and the ion density  $n$  are related to the measured  $V_f$  and  $I_{\text{sat}}$  through the relations  $V_p - V_f \approx a T_e$  and  $n \approx (m_i/T_e)^{0.5} I_{\text{sat}}$ , respectively.<sup>8</sup> Here,  $T_e$  is the electron temperature,

$(m_i/T_e)^{0.5}$  is the ion sound velocity in the plasma,  $m_i$  the ionic mass, and  $a=4$  is a parameter typical of our experimental setting.

The electron temperature fluctuations<sup>10</sup> at this pressure are below 15% along the whole plasma radius in the equatorial plane where measurements were performed. Plasma potential and density were calculated taking into account also the electron temperature fluctuations: The results we obtained showed that at the working pressure  $P=10^{-4}$  mbar, the electron temperature fluctuations do not give any significant contribution to the density and potential and, at least at this pressure, the electron temperature fluctuations  $T_e$  can be neglected.

To estimate the radial component of the plasma fluid velocity  $u_r$ , we assume that it is dominated by the  $u_{\vec{E} \times \vec{B}}$  drift velocity, where  $\vec{E}$  represents the poloidal electric field calculated as the difference between the two plasma potentials  $V_{p1}$  and  $V_{p2}$ . Under all stated approximations and assumptions, we estimate the fluid (as opposed to microscopic) particle flux in the radial direction at the instant  $t$  as the product  $\Gamma(t) = n(t) u_r(t)$ . Following the standard splitting procedure, we separate both  $n(t)$  and  $u_r(t)$  into average backgrounds  $\bar{n}$  and  $\bar{u}_r$ , and instantaneous fluctuations  $\tilde{n}(t)$  and  $\tilde{u}_r(t)$ , and then also the flux into a background flux  $\bar{\Gamma}$  and a fluctuating flux  $\tilde{\Gamma}(t)$ . In what follows, we will focus on the radial turbulent particle flux  $\tilde{\Gamma}(t)$  and, subsequently, on  $\tilde{n}(t)$  and  $\tilde{u}_r(t)$  separately.

### III. METHOD

We start off with a (stationary) discrete time-series for  $\Gamma(t_i)$  consisting of  $i=1, \dots, N_{\text{data}}$  ( $N_{\text{data}}=10000$ ) values, sampled at equal intervals  $\tau_{\text{data}}=4 \mu\text{s}$ , corresponding to a total time-span  $T=N_{\text{data}} \times \tau_{\text{data}}=0.04$  s.

The background flux  $\bar{\Gamma}$  is just the temporal average of  $\Gamma(t)$  over the total time-span  $T$ ,  $\bar{\Gamma}=T^{-1} \int_0^T \Gamma(t') dt' = \sum_i \Gamma(t_i) / N_{\text{data}}$ , and the instantaneous fluctuation at  $t$  is defined as  $\tilde{\Gamma}(t) = \Gamma(t) - \bar{\Gamma}$ . Following,<sup>6</sup> we calculate the coarse-grained function  $\Gamma_\tau(t)$  of  $\tilde{\Gamma}$  over nonoverlapping windows of length  $\tau$  as

$$\Gamma_\tau(t) = \frac{1}{\tau} \int_{t-\tau/2}^{t+\tau/2} dt' \tilde{\Gamma}(t'), \quad (1)$$

and the corresponding root mean square (rms) fluctuations

$$\sigma_\tau^2 = \frac{1}{T} \int_0^T dt' \Gamma_\tau^2(t'). \quad (2)$$

It follows that for the time scale  $\tau=T$ , i.e., for the whole sample length,  $\Gamma_\tau(t)=0$  and  $\sigma_\tau^2=0$ . Thus,  $\sigma_\tau$  is a decreasing function of  $\tau$ . Coarse-graining  $\tilde{\Gamma}$  over a scale  $\tau$  filters out all contributions to  $\sigma_\tau$  due to fluctuations over short time scales  $\tau_{\text{short}} \leq \tau$ . Since a given data sample has a fixed total length  $T$ , fluctuations over long time scales  $\tau_{\text{long}} \geq T$  are not present. One can think of  $\sigma_\tau^2$  as the “residual variance” due only to those fluctuations at frequencies between the variable “ultra-violet” (UV) cutoff  $\nu_{\text{UV}} \approx 1/\tau$  and the fixed “infrared” (IR)

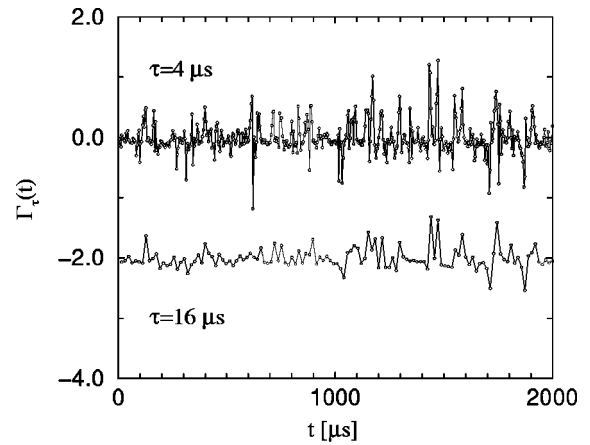


FIG. 1. Time series for the turbulent fluctuation particle flux  $\Gamma_\tau(t)$  vs  $t$  for (top) the original data corresponding to  $\tau=4 \mu\text{s}$ , and (bottom) the coarse-grained temporal resolution  $\tau=16 \mu\text{s}$ . Only part of the data has been plotted. The coarse grained series (bottom) has been downshifted by an amount of 2 for clarity.

cutoff  $\nu_{\text{IR}} \approx 1/T$ . In order to compare various  $\Gamma_\tau$  for different time scales  $\tau$ , it is convenient to define the standard variable  $g_\tau = \Gamma_\tau / \sigma_\tau$ . By definition,  $\bar{g}_\tau = 0$  and  $\bar{g}_\tau^2 = 1$ .

According to the above discussed method, we build a whole sequence of coarse-grained time-series  $\Gamma_\tau$  with corresponding coarser and coarser resolution  $\tau > 4 \mu\text{s}$ . A typical time-series and one of its coarse-grained time-series are shown in Fig. 1, for the radial position  $r=3.5$  cm from the center of the torus. Here, we are interested in the degree of fluctuation of  $\Gamma_\tau(t)$  around its mean. We consider then the histogram of data counts  $dN_\tau$  of  $\Gamma_\tau(t)$  within  $M_{\text{bin}}$  bins of equal (at given  $\tau$ ) width  $d_\tau \Gamma$ . We choose  $d_\tau \Gamma = 0.2 \sigma_\tau$ , yielding  $M_{\text{bin}} = 30$  bins within  $\pm 3 \sigma_\tau$ .

We define the count distribution function (CDF, normalized such that its total area equals  $N_\tau$ ) of  $\Gamma_\tau$  as the ratio,

$$\text{CDF}_\tau(\Gamma_\tau) = \frac{dN_\tau}{d_\tau \Gamma}. \quad (3)$$

The corresponding probability distribution function (PDF), whose total area is normalized to one, is defined as the ratio

$$\text{PDF}_\tau(\Gamma_\tau) = \frac{1}{N_\tau} \frac{dN_\tau}{d_\tau \Gamma}. \quad (4)$$

The resulting standard PDF is a function of the scaled variable  $g_\tau$ . It is customary to refer to the PDF as self-similar when its shape does not change with the temporal scale, and to self-affinity to a special form of statistical scaling of  $\Gamma_\tau$  with  $\tau$ , namely a power-law scaling of  $\sigma_\tau$  with an exponent  $\alpha$ ,  $\sigma_\tau \sim \tau^{-\alpha}$ , i.e.,

$$\frac{\sigma_{\tau_1}}{\sigma_{\tau_2}} = \left( \frac{\tau_1}{\tau_2} \right)^{-\alpha}. \quad (5)$$

The scaling exponent  $\alpha$  can also be expressed in terms of the so-called Hurst exponent  $H$  (see also Refs. 5 and 7 where a similar method for calculating  $H$  is discussed), according to  $\alpha = 1 - H$  and  $0 \leq H \leq 1$ , so that  $\alpha \rightarrow 0$  corresponds to  $H \rightarrow 1$  and  $\alpha = 1/2$  to the standard behavior  $H = 1/2$ . Values of

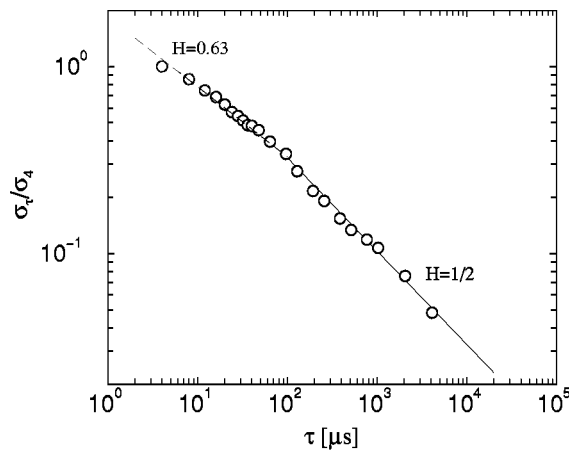


FIG. 2. Residual standard deviation  $\sigma_\tau/\sigma_4$  (open circles) as a function of  $\tau$  (in  $\mu s$ ), for the pressure of  $10^{-4}$  mbar and radial distance 3.5 cm. For illustration, we show two power laws  $\sigma_\tau \sim \tau^{-(1-H)}$  for  $H=0.63$  (dashed line) and  $H=1/2$  (continuous line) at short and long temporal resolutions, respectively.

$H > 1/2$  indicate persistence or positive correlations in the data, while  $H < 1/2$  antipersistence or anticorrelations. In many circumstances, however,  $\sigma_\tau$  does not display a single power-law behavior as in Eq. (5), but different values of the exponent  $\alpha$  can be found on different time scales (cf., e.g., Refs. 5 and 7).

#### IV. RESULTS AND DISCUSSION

##### A. Fluctuating flux

We have analyzed several flux time series as well as density and electric fields time series along the whole plasma diameter. Here we report data concerning turbulent flux, density and velocity fluctuations data of interest for transport and plasma confinement.

In Fig. 2 the standard deviation  $\sigma_\tau$  (corresponding to the data considered in Fig. 1) is shown as a function of the time scale  $\tau$ . It is possible to distinguish two main regimes where the standard deviation displays different behaviors. One regime is extending over many time decades, for time scales  $\tau > 100 \mu s$ , called *mesoscale* regime, while the other occurs at smaller time scales,  $\tau < 100 \mu s$ . This last regime is dominated by fast events and it is usually called *fluctuation* range. In this range, the standard deviation tends to display an approximate power law behavior with an effective exponent  $H > 1/2$ . The persistence associated to such values of  $H$  is due to the presence of short-range correlations in the time series, having a characteristic crossover time of the order of  $100 \mu s$ . For long time scales, i.e., for  $\tau > 100 \mu s$ , the standard deviation shows a clear power law with a Hurst exponent  $H \approx 0.5$ , indicating absence of correlations in the series. A similar behavior has been found also in the simple magnetized torus Thorello<sup>6</sup> and in other fusion-like devices.<sup>11,12</sup>

Looking in Fig. 3 at the CDF for different  $\tau$  it is possible to recognize that its shape deviates from a Gaussian, at least at short time scales. For longer time scales a progressive and gradual modification of the CDF can be appreciated towards

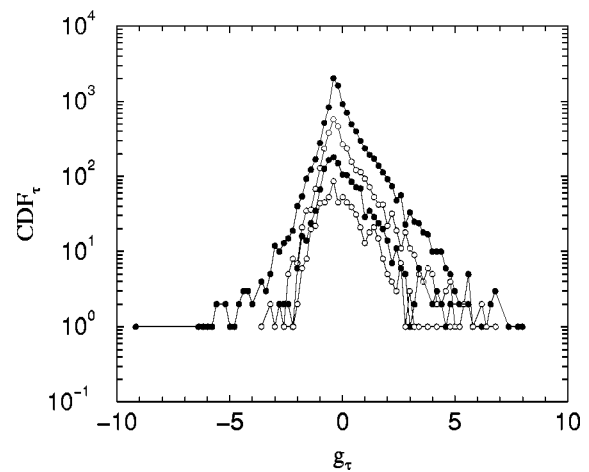


FIG. 3. CDF's as a function of the standard variable  $g_\tau$  for different time scales (from top to bottom):  $\tau = (4, 12, 28, 64) \mu s$ , for the pressure of  $10^{-4}$  mbar and radial distance 3.5 cm.

a Gaussian-type shape. The two regimes found in the standard deviation behavior seems to be reflected also on the CDF.

To estimate the degree of self-similarity and to elucidate more clearly deviations from the Gaussian distribution function, we have plotted the standard PDF in Fig. 4. As can be seen from Fig. 4, at short time scales the PDFs display a spiky shape and fat tails describing outward fluxes [Fig. 4(a)]. Notice that the non-Gaussian scaling of the standard deviation (having  $H > 0.5$ ) does not imply necessarily that the PDF should be also non-Gaussian. Cases are known, e.g., fractional Brownian motion,<sup>13</sup> for which the PDF has indeed a Gaussian shape while its variance scales anomalously with time (i.e.,  $H \neq 1/2$ ). Since  $\sigma_\tau$  is finite for all  $\tau$ , the central limit theorem (CLT) tells us that the PDF will gradually turn into a Gaussian-type distribution for increasing time scales  $\tau$ . As shown in Fig. 4(b), however, this transition is rather slow in Blaamann as compared, e.g., to Thorello.<sup>6</sup> The mesoscale regime is characterized by a Hurst exponent  $H \approx 0.5$  for all the plasma radii (cf. Fig. 5). The randomization of transport events in the mesoscale regime is, therefore, systematically present along the entire equatorial plasma radius. In the case of Blaamann the corresponding PDF's still display significant deviations from the standard Gaussian shape.

Regarding the short time scale, the latter seems to be related to events involving the dynamics of long lived structures. In fact, coherent structures of vortex type have been recently detected in Blaamann in helium plasma.<sup>14</sup> The typical evolution time of these structures is of the order of  $10 \mu s$ , and the time for a total revolution in the poloidal plasma cross section is about  $100 \mu s$ , as can be seen in Sec. IV C below. Thus, in the short time scale  $\tau < 100 \mu s$ , the strong non-Gaussianity is related to the presence of coherent structures and the transport, i.e., the instantaneous flux, is dominated by their dynamics.

##### B. Density and velocity fluctuations

It is also interesting to observe that the behavior of the velocity and density PDF as well their standard deviations

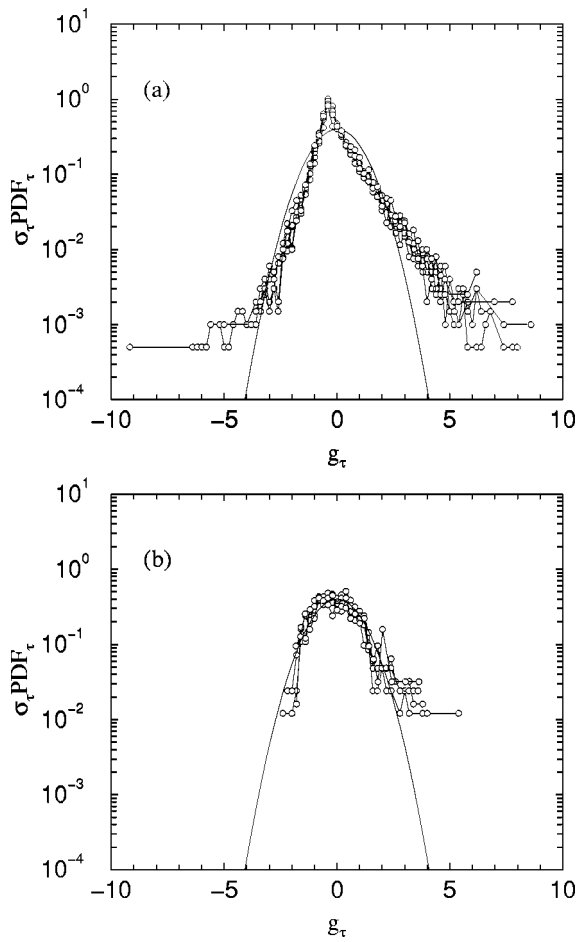


FIG. 4. Standard probability distribution functions,  $\sigma_\tau \text{PDF}_\tau$ , of turbulent flux fluctuations  $\Gamma_\tau$  for different coarse-grained temporal resolutions  $\tau$ , plotted as a function of  $g_\tau$ : (a) Short time resolutions  $\tau = (4, 8, 12, 16, 20) \mu\text{s}$  (“fluctuation range”); (b) long time resolutions  $\tau = (96, 128, 192, 256) \mu\text{s}$  (“mesoscale range”), for the pressure of  $10^{-4}$  mbar and radial distance 3.5 cm. For comparison, we show the standard Gaussian distribution.

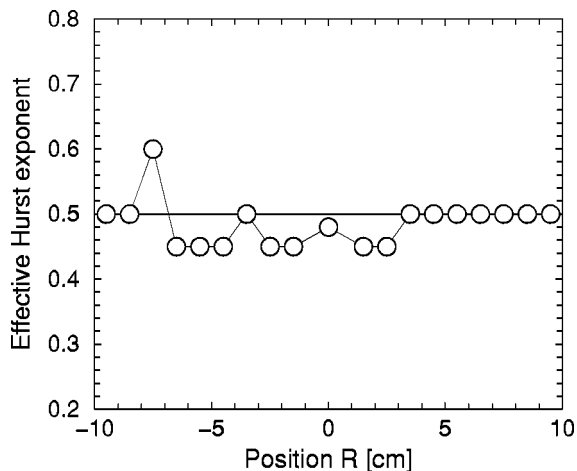


FIG. 5. Effective Hurst exponent in the mesoscale regime ( $\tau > 100 \mu\text{s}$ ) as a function of the radial position  $R$  in Blaumann, for the fluctuation flux (open squares), for the pressure of  $10^{-4}$  mbar. The error bars are estimated to be about 10%.

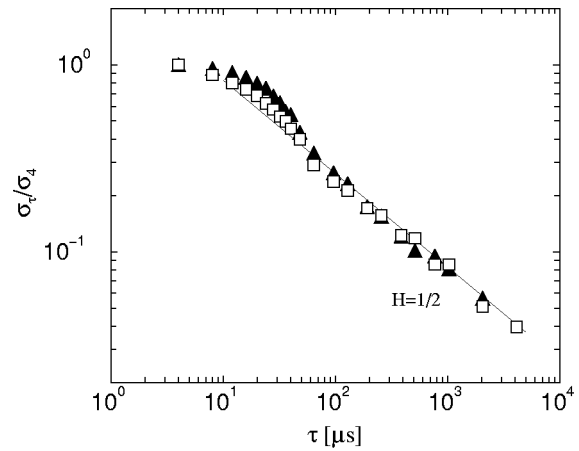


FIG. 6. Residual standard deviation  $\sigma_\tau/\sigma_4$  as a function of  $\tau$  (in  $\mu\text{s}$ ) for the radial velocity (full triangles) and density fluctuations (open squares), for the pressure of  $10^{-4}$  mbar and radial distance 3.5 cm. For illustration, we show the power law  $\sigma_\tau \sim \tau^{-(1-H)}$  for  $H = 1/2$  (continuous line) at long temporal resolutions.

are different from what found for the flux ones. As can be seen from Fig. 6, the standard deviations are characterized by a Hurst exponent consistent with the standard value  $H = 1/2$  for long time scales, extending, however, to values of  $\tau$  smaller than  $100 \mu\text{s}$ . At  $\tau < 10 \mu\text{s}$ , the exponent tends to flatten, while the transition to the  $H = 1/2$  regime, occurring around  $100 \mu\text{s}$ , is more pronounced than in the case of the flux.

In addition, the strong asymmetry in the PDF and its deep peak found for the fluxes in the fluctuation range do not appear in the PDF neither of velocity nor of density fluctuations. As can be seen from Fig. 7, the PDF of both velocity and density fluctuations are more Gaussian-like. Then the velocity and density PDF, as shown in Fig. 7, although deviate from a Gaussian distribution, are not peaked as the flux PDF. The analysis of the Hurst exponent as a function of the radial position is shown in Fig. 8 for the density and velocity fluctuations. For the velocity,  $H$  is found to be near 0.5 along the whole torus diameter, while for the density it detaches from the standard value 0.5 near the high field zone. The behavior of the density is anomalous with respect to the velocity and the flux ones.

It is then important at this point to mention that the physics and statistical properties of the transport events, that is of the PDF fluxes, depend strictly on the correlation of velocity and density and not only on one of them or both independently. Then, large transport events at small time scales seem to be regulated by complex processes involving directly the local correlation between velocity and density which in turn is a consequence of the complex dynamics of spatially delocalized large structures.

Another point concerns self-similarity properties of the PDF. Applying statistical tests described in detail in Ref. 6, it appears that in the two regimes the distribution is self-similar. But a more important issue is that in the mesoscale range flux and velocity fluctuations are Gaussian distributed and randomised and no long-time correlations occur. However, also the work of Ref. 4 concerning a statistical analysis

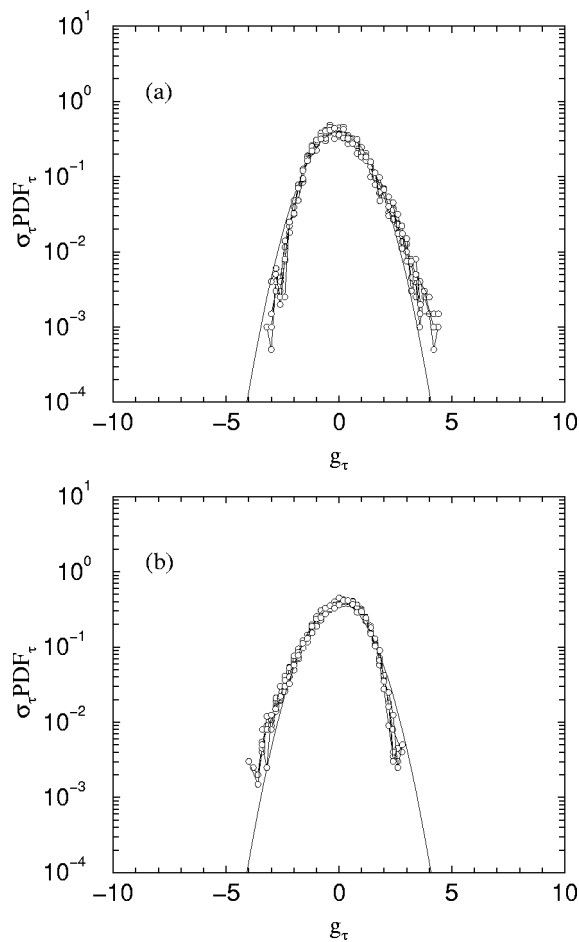


FIG. 7. Standard probability distribution functions,  $\sigma_\tau \text{PDF}_\tau$ , of (a) radial velocity fluctuations and (b) density fluctuations, plotted as a function of  $g_\tau$ , for different coarse-grained temporal resolutions  $\tau = (4, 8, 12, 16, 20) \mu\text{s}$ , for the pressure of  $10^{-4}$  mbar and radial distance 3.5 cm. In both cases we show, for comparison, the standard Gaussian distribution.

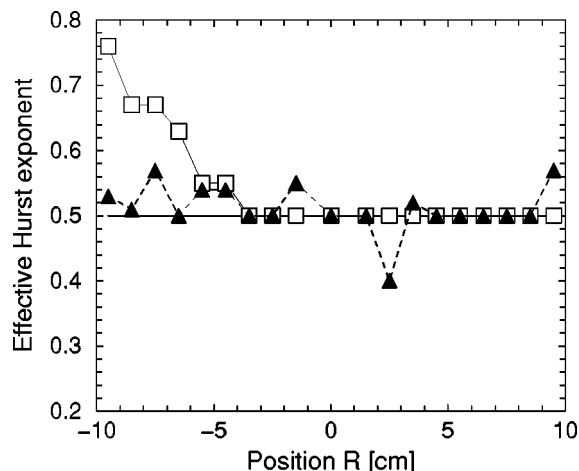


FIG. 8. Effective Hurst exponent in the mesoscale regime ( $\tau > 100 \mu\text{s}$ ) as a function of the radial position  $R$  in Blaamann, for the electronic density (open squares) and the velocities (full triangles), for the pressure of  $10^{-4}$  mbar. The error bars are about 10%.

of ion saturation current applied to the Tore Supra fusion device indicates that no long-time correlations occur in the mesoscale regime, even if, in this regime, the Hurst exponent seems to be greater than 0.5. These results suggest that the absence of long range correlations in the mesoscale regime is not only peculiar of nonfusion devices.

Recently, some indications have been given that in Blaamann, Hurst exponents larger than 1/2 are obtained in the mesoscale regime by studying time series of the plasma potential.<sup>15</sup> To investigate whether our samples also present such anomalies, we have systematically performed the coarse-grained analysis for the density and velocity fluctuations time series over the whole range of radial distances. The results for the effective Hurst exponents, obtained from power law fits of the corresponding standard deviations in the mesoscale regime, are summarized in Fig. 8. As one can see, density fluctuations display long time anomalous decay for distances  $R < -4$  cm, with effective  $H$  as large as 0.7–0.8, while velocity fluctuations are consistent, within the statistical errors, with a more standard decay over the whole range of radial distances. For distances  $R > -4$  cm, density fluctuations behave in the standard way. Details of these analysis will be published elsewhere.

**C. The presence of coherent structures in Blaamann**

A very important issue regards the possible universal behavior of turbulent transport in plasma devices. Results obtained on Blaamann are very similar not only to those obtained from a similar device Thorello, but are also similar to fusion devices ones, like for instance the Wendelstein 7 Advanced Stellarator (W7-AS) plasma-fusion device.<sup>12,16</sup> That is, in general, there are two distinct time scale regimes, the fluctuating range and the mesoscale one, for which the behavior of the standard deviation is very similar, although the Hurst exponent in the mesoscale regime is different between fusion and nonfusion devices. In the case of Blaamann, the time scale at which the crossover between the fluctuation and the mesoscale regime takes place can be associated to the decay of coherent structures in the plasma. Indeed, as indicated in Fig. 9, coherent structures seem to persist over time scales of the order of 100  $\mu\text{s}$ , corresponding roughly to the revolution time being of the order of 100  $\mu\text{s}$ .

**V. CONCLUSIONS**

In the statistical analysis performed in the simple magnetized torus Blaamann, we found some specific issues related to the transport properties but also some more general properties of turbulence in comparison with the performed analysis in other fusion and nonfusion devices. We found some universalities in the behavior of the PDF and its standard deviation for what concerns the existence of two time scale regimes. One is the short time scale, in which the standard deviation displays an approximate power law with Hurst exponent larger than 1/2 and the PDF, having a strongly asymmetric peaked distribution, departs strongly from a Gaussian behavior. The other is the long time scale, in which the standard deviation follows a power law as a function of time with  $H \approx 0.5$  and the PDF displays a more

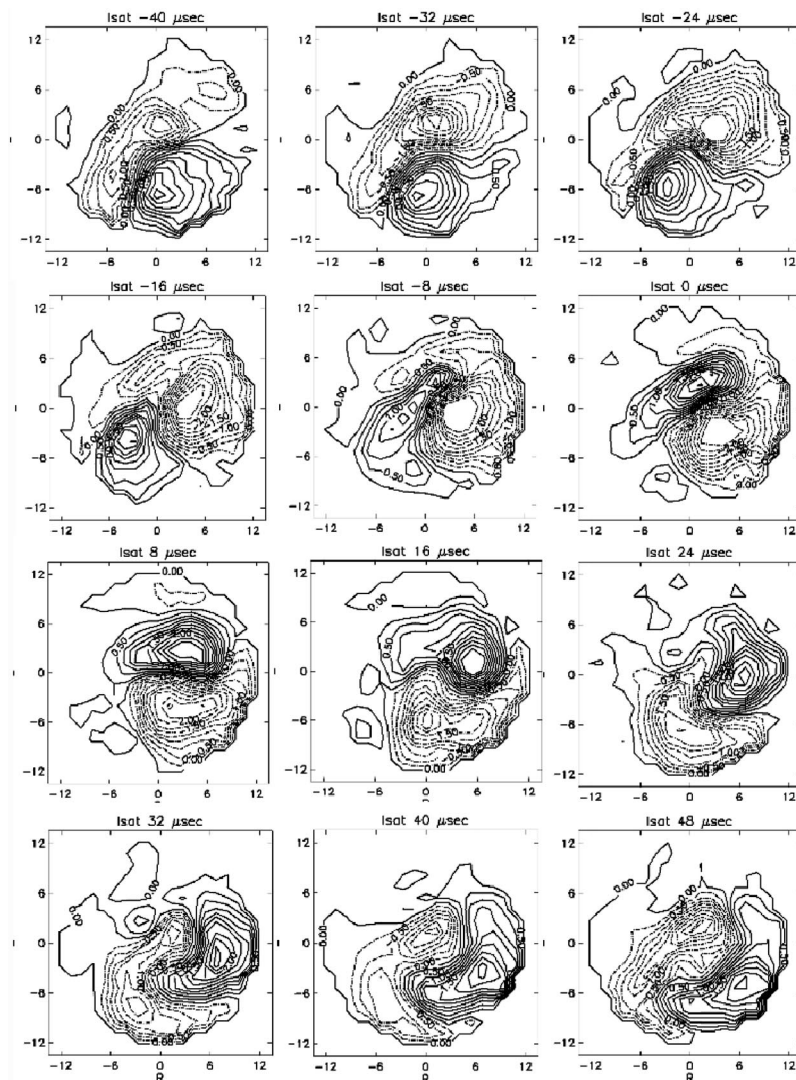


FIG. 9. Contour plots of the observed coherent structures in Blaamann derived from the electron saturation current. The values of  $R$  are in cm on both axes.

Gaussian-like distribution. This behavior is the result of the CLT, and is very similar to that found in fusion devices,<sup>1-3,11,12</sup> as well as in similar nonfusion devices.<sup>6</sup> More specifically, in the short time scale the dynamics of coherent structures dominates the transport in Blaamann. In fact, we found that at short time scales events are well represented by the dynamical evolution of vortical structures in the plasma poloidal cross section. The departure from Gaussianity in the PDF is, therefore, related to the presence of long lived structures. Another important point is that transport statistical characteristics are dominated by the correlation of density and potential and not simply by the statistical properties of each of them. The latter result outlines how transport processes are complex.

<sup>1</sup>B. A. Carreras, B. van Milligen, M. A. Pedrosa, R. Balbin, C. Hidalgo, D. E. Newman, E. Sanchez, M. Frances, E. Garcia-Cortes, J. Bleuel, M. Endler, C. Riccardi, S. Davies, G. F. Matthews, E. Martines, V. Antoni, A. Latten, and T. Klinger, *Phys. Plasmas* **5**, 3632 (1998).

<sup>2</sup>B. A. Carreras, B. van Milligen, C. Hidalgo, R. Balbin, E. Sanchez, E. Garcia-Cortes, M. A. Pedrosa, J. Bleuel, and M. Endler, *Phys. Rev. Lett.* **83**, 3653 (1999).

<sup>3</sup>G. Wang, G. Y. Antar, and P. Devynck, *Phys. Plasmas* **7**, 1181 (2000).

<sup>4</sup>G. Y. Antar, P. Devynck, X. Garbet, and S. C. Luckhardt, *Phys. Plasmas* **8**, 1612 (2001).

<sup>5</sup>M. Gilmore, C. X. Yu, T. L. Rhodes, and W. A. Peebles, *Phys. Plasmas* **9**, 1312 (2002).

<sup>6</sup>R. Trasarti-Battistoni, D. Draghi, C. Riccardi, and H. E. Roman, *Phys. Plasmas* **9**, 3369 (2002).

<sup>7</sup>C. X. Yu, M. Gilmore, W. A. Peebles, and T. L. Rhodes, *Phys. Plasmas* **10**, 2772 (2003).

<sup>8</sup>C. Riccardi and A. Fredriksen, *Phys. Plasmas* **8**, 199 (2001).

<sup>9</sup>F. J. Øynes, O. M. Olsen, H. L. Pécseli, A. Fredriksen, and K. Rypdal, *Phys. Rev. E* **57**, 2242 (1998).

<sup>10</sup>A. Fredriksen, C. Riccardi, and G. Longoni, *Rev. Sci. Instrum.* **72**, 457 (2001).

<sup>11</sup>B. A. Carreras, B. van Milligen, M. A. Pedrosa, R. Balbin, C. Hidalgo, D. E. Newman, E. Sanchez, R. Bravenec, G. McKee, E. Garcia-Cortes, J. Bleuel, M. Endler, C. Riccardi, S. Davies, G. F. Matthews, E. Martines, and V. Antoni, *Phys. Plasmas* **6**, 1885 (1999).

<sup>12</sup>B. A. Carreras, V. E. Lynch, D. E. Newman, R. Balbin, J. Bleuel, M. A. Pedrosa, M. Endler, B. van Milligen, E. Sanchez, and C. Hidalgo, *Phys. Plasmas* **7**, 3278 (2000).

<sup>13</sup>J. Feder, *Fractals* (Plenum, New York, 1988).

<sup>14</sup>A. Fredriksen, C. Riccardi, L. Cartegni, and H. L. Pécseli, *Plasma Phys. Controlled Fusion* **45**, 721 (2003).

<sup>15</sup>K. Rypdal and S. Ratynskaia, *Phys. Plasmas* **10**, 2686 (2003).

<sup>16</sup>J. Bleuel, G. Theimer, M. Endler *et al.*, in *Controlled Fusion and Plasma Physics* (European Physical Society, Petit Lancy, 1996), Vol. 20C, p. 727.